JOURNAL OF INTERFERON & CYTOKINE RESEARCH
Volume 43, Number 9, 2023

DOI: 10.1089/jir.2023.0046

Deletion of Interferon Lambda Receptor Elucidates Susceptibility to the Murine Model of Biliary Atresia

Stephen J. Hartman,[1] Madeleine A. Weiss,[1] Haley M. Temple,[1] Bryan Donnelly,[1] Rajamouli Pasula,[1] Holly M. Poling,[1] Monica McNeal,[1] Sujit K. Mohanty,[2] and Greg M. Tiao[1]

Biliary atresia (BA) is a life-threatening cholangiopathy occurring in infancy, the most common indication for pediatric liver transplantation. The etiology of BA remains unknown; however, a viral etiology has been proposed as multiple viruses have been detected in explants of infants afflicted with BA. In the murine model of BA, Rhesus rotavirus (RRV) infection of newborn BALB/c pups results in a cholangiopathy that mirrors human BA. Infected BALB/c pups experience 100% symptomatology and mortality, while C57BL/6 mice are asymptomatic. Interferon-λ (IFN-λ) is an epithelial cytokine that provides protection against viral infection. We demonstrated that IFN-λ is highly expressed in C57BL/6, leading to reduced RRV replication. RRV-infection of C57BL/6 IFN-λ receptor knockout (C57BL/6 IFN-λR KO) pups resulted in 90% developing obstructive symptoms and 45% mortality with a higher viral titer in bile ducts and profound periportal inflammation compared to C57BL/6. Histology revealed complete biliary obstruction in symptomatic C57BL/6 IFN-λR KO pups, while C57BL/6 ducts were patent. These findings suggest that IFN-λ is critical in preventing RRV replication. Deficiency in IFN-λ permits RRV infection, which triggers the inflammatory cascade causing biliary obstruction. Further IFN-λ study is warranted as it may play an important role in infant susceptibility to BA.

Keywords: biliary atresia, interferon-λ, type III interferon, rhesus rotavirus, cholangiocytes

Introduction

Biliary atresia (BA) is a rare, but life-threatening obliterative cholangiopathy that occurs in the first few months of life, varying in frequency from 1 in 8,000 to 15,000 live births per year (Yoon and others 1997; Davenport 2005). Without surgical drainage via Kasai portoenterostomy or liver transplantation, BA is universally fatal (Kasai 1959; Hopkins and others 2017). The etiology of BA remains unknown, though several hypotheses have been proposed including viral infection as evidenced by the presence of virus in the explanted livers of BA patients [cytomegalovirus (CMV), reovirus, rotavirus, Human Papilloma Virus, Epstein–Barr virus (EBV)] (Tyler and others 1998; Asai and others 2015; Zani and others 2015; Lakshminarayanan and Davenport 2016). A viral infection initiates an inflammatory cascade, leading to immune cell recruitment, activation, biliary epithelial injury, and subsequent obstruction (Ohya and others 1995; Mack and others 2007; Erickson and others 2008).

Newborn BALB/c mouse pups injected intraperitoneally with rhesus rotavirus (RRV) develop symptoms of biliary obstruction consistent with human BA patients including jaundice, hyperbilirubinemia, and acholic stools (Mohanty and others 2019, 2020). We have previously demonstrated that RRV replicates at high levels in the bile duct and liver (Allen and others 2007; Mohanty and others 2013). Histopathology demonstrates significant periportal inflammation and bile duct obstruction paralleling the human disease (Riepenhoff-Talty and others 1993; Davenport and others 2001).

Previous studies have shown that mouse lines vary significantly in their susceptibility to infection and immune response (Simpson and others 1997; Santos and others 2010;

[1]Department of Pediatric and Thoracic Surgery, Cincinnati Children's Hospital Medical Center, Cincinnati, Ohio, USA.
[2]Southeast Poultry Research Laboratory, US National Poultry Research Center, United States Department of Agriculture (USDA-ARS), Athens, Georgia, USA.

Sellers and others 2012). For example, the C57BL/6 mouse line typically elicits a stronger Th1 response, whereas BALB/c mice exhibit a predominant Th2 response, making BALB/c mice more dependent on cytokines released by antigen-presenting cells for innate immunity (Mills and others 2000). These different strains of mice also produce immune cells and their cytokines in varying quantities, affecting their ability to respond to infection. Because of their Th1 bias, C57BL/6 mice have more dominant cell-mediated immunity, which is evidenced by their resistance to infection with intracellular pathogens (Elkins and others 2002). The murine model of BA is unique to the BALB/c mouse line, suggesting a unique strain-specific aspect of its host response to infection that may be playing a role in the pathogenesis of murine BA. We sought to investigate this by using knockout mice in a known mouse strain that has been previously resistant to the murine BA model.

Interferon-λ (IFN-λ), also known as type III IFN, is a member of the IFN family of cytokines involved in innate immunity and host defense. IFN-λ is preferentially expressed in the epithelial cells of both humans and mice (Ye and others 2019). Previous work has demonstrated that IFN-λ plays a critical role in the host defense against several viruses both in the respiratory and intestinal epithelium acting as a paracrine cytokine, signaling surrounding cells after viral exposure, and protecting against subsequent infection of neighboring cells. This has been observed with influenza A virus, CMV, herpes simplex virus type 1, EBV, and rotavirus in epithelial cells (Brand and others 2005; Jewell and others 2010; Muzammil and others 2017; Doldan and others 2022). Additionally, IFN-λ has been shown to be protective of reovirus infection in the cholangiocytes of the bile duct (Mahlakõiv and others 2015).

Mouse cholangiocytes are unique as they are the only cell in the mouse liver that is responsive to IFN-λ (Hermant and others 2014). Given these findings, we sought to evaluate IFN-λ's role in the prevention of RRV replication and the development of the murine model of BA.

Materials and Methods

Animals, cells, and virus

BALB/c and C57BL/6 mice were obtained from Envigo Labs (Indianapolis, IN). C57BL/6 mice knocked out for the IFN-λ receptor (C57BL/6 IFN-λR KO) were kindly provided by Dr. Sergei Kotenko (*Ifnlr1*$^{tm1.2Svko}$, 6200891; MGI) (Department of Microbiology, Biochemistry, and Molecular Genetics, Rutgers University, Newark, NJ) (Lin and others 2016). All animal research was performed in accordance with regulations and protocols approved by the Institutional Animal Care and Use Committee at Cincinnati Children's Hospital Medical Center (Protocol no. IACUC 2022-0048), which follows the National Institutes of Health OLAW regulation (Animal Assurance no. A3108) and the Animal Welfare Act (certification no. 31-8-001).

MA104 cells (BioWhittaker, Walkersville, MD) were grown in Dulbecco's modified Eagle's medium (DMEM) (Cellgro) containing 10% fetal bovine serum (FBS) (Gibco/BRL, Gaithersburg, MD), 0.01% penicillin-streptomycin (Gibco/BRL), 0.01% L-glutamine (Gibco/BRL), and 0.005% amphotericin B (Cellgro), as described (Jafri and others 2008; Mohanty and others 2013).

The rotavirus strain RRV generously provided by Dr. Harry Greenberg (Stanford University, Palo Alto, CA) was propagated in MA104 cells as previously described (Mohanty and others 2019).

Murine model of BA

Newborn pups were injected intraperitoneally with RRV at 1.5×10^6 focus-forming units (FFU) per pup. The mice were monitored for 21 days for clinical signs of hepatobiliary injury (ie, acholic stools, bilirubinuria, and jaundice in bare skin) along with survival. Mice were recorded as symptomatic if they met two of these previously described symptoms. Subsets of these mice had their extrahepatic bile duct and liver harvested at various time points for viral titers and histology.

Isolation of primary murine cholangiocytes

On day of life (DOL) 2, primary cholangiocytes were harvested from noninfected neonatal BALB/c and C57BL/6 pups. Livers were extracted, homogenized, and subsequently digested with DMEM/Nutrient Mixture F-12 (F12) supplemented with L-glutamine, penicillin, streptomycin, heat-inactivated FBS (Invitrogen, Waltham, MA), collagenase, hyaluronidase, and DNase I (Sigma-Aldrich, St. Louis, MO). After incubation for 1 h at 37°C, the digestate was filtered (40 μm), collected, and purified with a Percoll gradient (GE Healthcare, Sweden).

The filtered cells were washed, pelleted, and then suspended in phosphate-buffered saline (PBS) (Gibco) supplemented with 0.1% bovine serum albumin (BSA) and incubated at 4°C with an Ep-CAM antibody (Developmental Studies Hybridoma Bank, The University of Iowa, Iowa City, IA). The cells were washed, suspended in PBS +0.1% BSA, and mixed with sheep anti-rat Dynabead IgG antibodies (Invitrogen) at 4°C. Dynabead-coated cells were magnetically purified, suspended in cholangiocyte media then plated on collagen-coated T25 cell culture flasks (Becton Dickinson, Franklin Lakes, NJ), and incubated at 37°C in 5% CO_2 until 80%–100% confluency.

Infection of primary cholangiocytes. The previously described primary cholangiocytes were seeded in 24-well plates in DMEM/F12 and incubated at 37°C until 90% confluence as previously described (Mohanty and others 2013). These cholangiocytes were then washed with Earles' balanced salts solution and subsequently infected with RRV at a multiplicity of infection (MOI) of 1 at 37°C for 1 h. At this MOI, the cells were infected at a 1:1 ratio with viral replicates. The plates were then washed and incubated with serum-free (SF) DMEM/F12 at 37°C for 24 h, and viral titers were quantified by focus-forming assay (FFA).

Quantification of infectious rotavirus

Infectious rotavirus was quantified by FFA as previously described (McNeal and others 1994; Mohanty and others 2019). MA104 cells were placed on 96-well plates and subsequently incubated at 37°C to confluency. These cells were infected with serially diluted RRV for 1 h at 37°C. The cells were washed, overlaid with DMEM supplemented with 4 μg/mL of trypsin, and incubated for 14–16 h. The cells were fixed with cold acetone (80%, 15 min, −20°C), and then guinea pig anti-rotavirus immunoglobulin G (IgG)

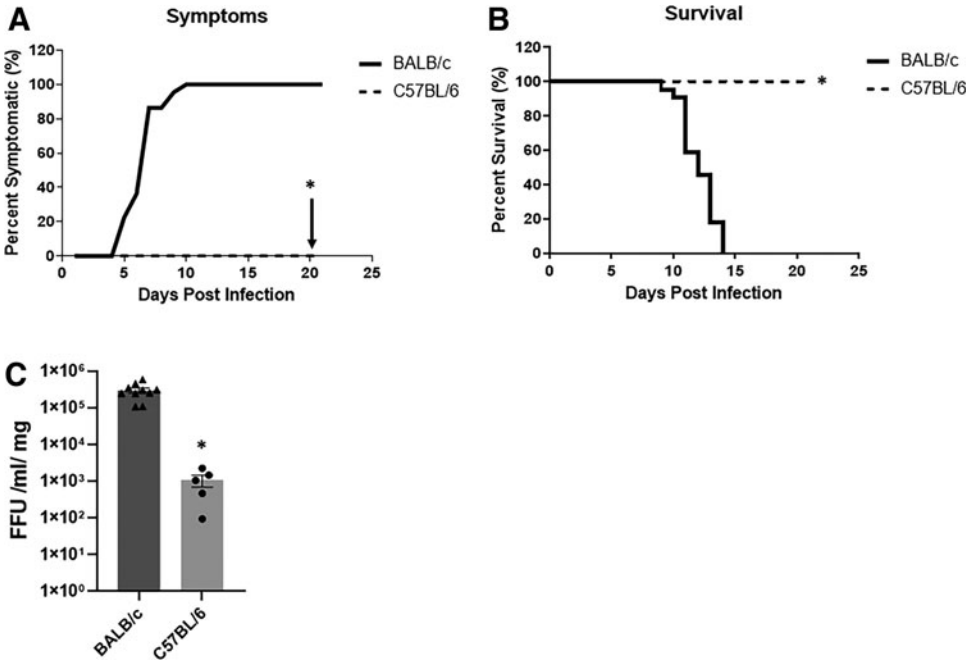

FIG. 1. RRV replication, symptoms, and survival in BALB/c and C57BL/6 mice. **(A)** 100% of BALB/c mice ($n=22$) were symptomatic following RRV infection compared with C57BL/6 mice ($n=19$), which did not develop symptoms. Fisher's exact test $^*P<0.05$. **(B)** BALB/c mice demonstrated 100% mortality within 21 days, compared to 0% mortality in the C57BL/6 line. Fisher's exact test $^*P<0.05$. **(C)** C57BL/6 mice ($n=5$) at 7 DPI have significantly lower RRV titer in the bile duct compared to BALB/c mice ($n=10$). Unpaired *t*-test $^*P<0.05$. Triangles represents BALB/c. Circles represents C57BL/6. DPI, days postinfected; RRV, rhesus rotavirus.

antibody (1:1,000) was added for a 30-min incubation period. Wells were washed with PBS, and fluorescein isothiocyanate-tagged goat anti-guinea pig IgG antibody (1:500) was added for 30 min at 37°C. After washing, infectious virus was quantified using UV microscopy (10× objective). This was recorded as FFU per milliliter.

Quantification of IFN-λ by Western blot analysis and ELISA

Serum from 2-day old BALB/c and C57BL/6 mice as well as media from primary cholangiocytes before and after a 24-h incubation period in SF media with and without virus were diluted in 5× loading buffer, ran on a 4%–20% tris-glycine gel (Invitrogen), transferred to polyvinylidene difluoride membranes (GE Healthcare, Pittsburgh, PA), and blocked with 5% milk solution. IFN-λ was evaluated on membranes with rabbit anti-IL-28/IL-29 antibody (1:1,000 dilution) (Abcam, Waltham, MA) and mouse anti-Actin antibody (1:5,000 dilution) (Seven Hills Bioreagents, Cincinnati, OH) as a loading control. Blots were imaged using a Bio-Rad ChemiDoc MP (Bio-Rad Laboratories, Hercules, CA). Densitometry was used to quantify levels of IFN-λ and compare between groups.

ELISA was performed on the same samples according to the manufacturer's instructions of the RayBio® Mouse IL-28A/B ELISA Kit (RayBiotech, Norcross, GA). Serum and supernatant samples were diluted 1:20 and 1:5, respectively. The optical density was obtained using a Biotek Synergy H1 microplate reader (Agilent, Santa Clara, CA) set to 450 nm. Concentrations were calculated with Biotek Gen5 v3.04 (Agilent).

Statistical analysis

Continuous variables were expressed as means ± standard error and evaluated by analysis of variance with *post hoc* testing, where appropriate. A P value <0.05 was considered significant. All statistical analysis was completed using Prism 9 (GraphPad Software, Inc., La Jolla, CA).

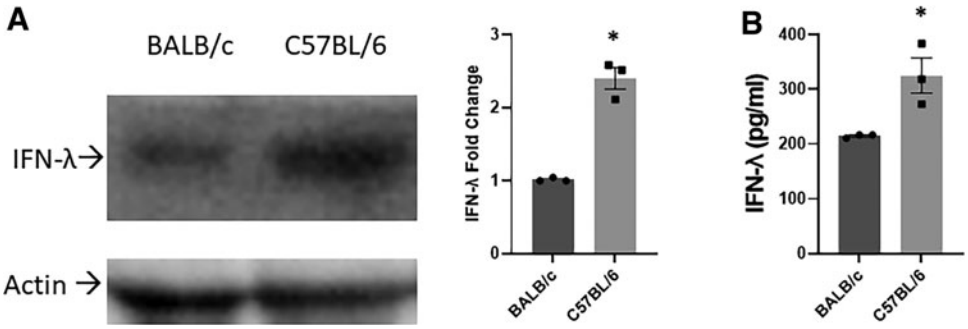

FIG. 2. Western blot analysis and ELISA of IFN-λ in the serum of noninfected mice. **(A)** Serum obtained from DOL 2 saline-injected C57BL/6 mice demonstrated 2.5-fold higher levels of constitutive IFN-λ compared to BALB/c mouse serum as determined by Western blot. **(B)** Protein levels were confirmed by ELISA ($n=3$ per mouse strain). Unpaired *t*-test $^*P<0.05$. Circle represents BALB/c. Square represents C57BL/6. DOL, day of life; IFN-λ, interferon-λ.

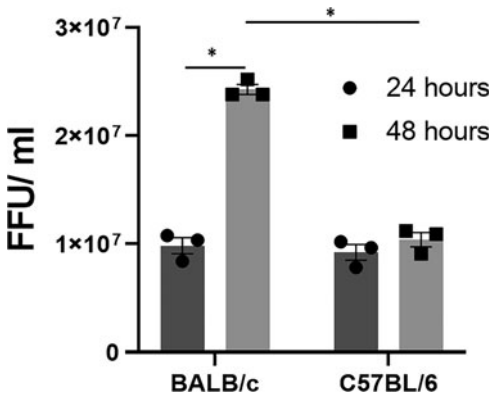

FIG. 3. RRV replication in primary cholangiocytes at 24- and 48-h postinfection. RRV titers from day 2 primary cholangiocytes were similar between BALB/c and C57BL/6 mice at 24 h following infection with multiplicity of infection of 1. At 48 h postinfection, BALB/c cholangiocytes demonstrated a significant increase in viral replication, while C57BL/6 cholangiocytes had no significant change in viral titer ($n=3$ wells per time point per cell line, experiment repeated 3 times). Two-way ANOVA $*P<0.05$. ANOVA, analysis of variance.

Results

Characterization of in vivo infection of mouse strains

We have previously demonstrated that BALB/c mice develop bile duct obstruction when injected with RRV within 24 h of birth (Shivakumar and others 2004; Allen and others 2007; Jafri and others 2009). Following RRV infection, BALB/c mice developed symptoms of biliary obstruction by DOL 7–10, while C57BL/6 mice expressed no symptoms over the 21-day study period (Fig. 1A). At 21 days, BALB/c mice experienced 100% mortality, while all C57BL/6 mice survived (Fig. 1B).

To determine if viral load was contributing to the BA phenotype, we evaluated the amount of live virus present within the bile ducts from 7 days postinfected (DPI) mice, the primary target of RRV (Jafri and others 2008). BALB/c bile ducts demonstrated significantly higher quantities of infectious RRV compared to the C57BL/6 mice (Fig. 1C).

We next sought to compare levels of IFN-λ *in vivo*. Serum obtained from noninfected C57BL/6 and BALB/c mouse pups on DOL 2 revealed a 2.5-fold higher level of IFN-λ in C57BL/6 mice compared to BALB/c mice as illustrated by Western blot and confirmed by ELISA (Fig. 2A, B). This demonstrated that neonatal C57BL/6 mice have constitutively higher levels of IFN-λ in their sera compared to BALB/c mice.

Comparison of infection in primary cholangiocytes of different mouse strains

To understand if this increase in viral titers was due to direct infection of the bile duct, primary cholangiocytes were isolated from day 2 old BALB/c and C57BL/6 pups and infected with RRV. FFA performed on these cholangiocytes at 24 and 48 h demonstrated similar titers of infectious RRV at 24 h postinfection. At 48 h, RRV viral titers increased more than twofold in BALB/c cholangiocytes, while C57BL/6 viral titers remained relatively constant (Fig. 3).

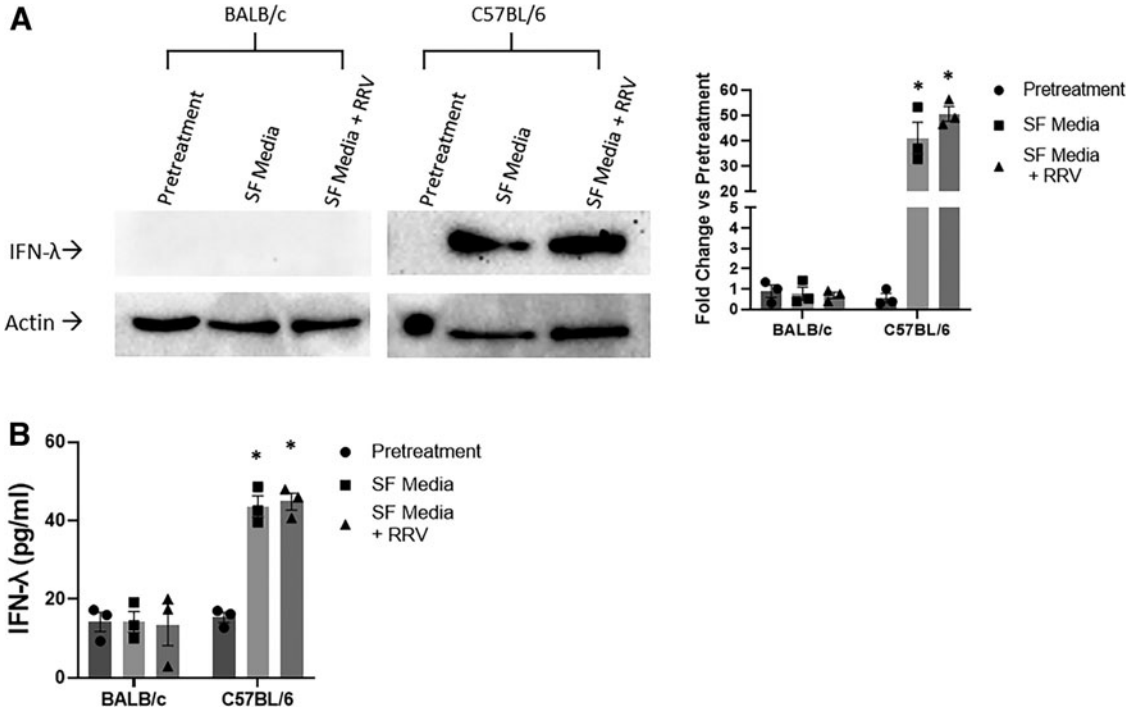

FIG. 4. Western blot analysis of IFN-λ from primary cholangiocytes with and without infection. **(A)** IFN-λ levels were significantly higher in C57BL/6 primary cholangiocyte supernatant both with RRV infection and serum-free media alone at 24 h when compared to supernatant from cells before treatment while no difference was witnessed in primary cholangiocytes isolated from BALB/c mice, quantified by densitometry and **(B)** confirmed by ELISA ($n=3$, repeated 3 times). Two-way ANOVA $*P<0.05$.

Primary cholangiocytes were infected with RRV and underwent analysis for IFN-λ release. IFN-λ levels were significantly elevated in C57BL/6 mouse cholangiocytes both after infection and SF media alone but were nearly undetectable before treatment or in the BALB/c cholangiocytes after treatment (Fig. 4).

Characterization of RRV infection in vivo

Given that BALB/c mice had lower levels of IFN-λ, we evaluated RRV replication in C57BL/6 IFN-λR KO pups. Bile ducts harvested on 7 DPI revealed RRV in both lines; however, titers were significantly higher in bile ducts from C57BL/6 IFN-λR KO mice when compared to C57BL/6 (Fig. 5A).

Following RRV infection, 90% of C57BL/6 IFN-λR KO mice developed symptoms of BA. This was significantly increased compared with the C57BL/6 pups (Fig. 5B). At 21 days, there was 45% mortality in C57BL/6 IFN-λR KO mice contrasting with 100% survival in wild-type mice (Fig. 5C).

Immunohistochemistry performed on liver sections of 7 DPI pups demonstrated that there was no positive staining for RRV antigens within C57BL/6, whereas RRV antigens were evident in the portal triad of C57BL/6 IFN-λR KO mice (Fig. 6). These findings are consistent with our previously reported data in the BALB/c line (Allen and others 2007).

To determine if this increased infection had an effect on the hepatobiliary system, histology was performed on livers of 10 DPI in C57BL/6 and C57BL/6 IFN-λR KO mice. C57BL/6 pups demonstrated minimal inflammation, consistent with saline controls, while C57BL/6 IFN-λR KO mice displayed significant inflammation within the portal triads (Fig. 7A). Histological evaluation of the extrahepatic bile ducts confirmed that the C57BL/6 were all patent, whereas those from RRV-infected C57BL/6 IFN-λR KO mice displayed complete obstruction in all symptomatic mice (Fig. 7B).

Discussion

BA is a disease unique to infancy, occurring in the first 6 months of life (Sanchez-Valle and others 2017). The temporal nature of BA suggests that there is an aspect in infant immunology and/or physiology that makes them susceptible to the disease process. We have previously shown that infection with RRV in older mice fails to induce murine BA, suggesting that the murine model of BA has a temporal dependence which parallels the human disease (Mohanty and others 2013). We have found that the murine model is specific to the BALB/c strain without a biological explanation as to why other mouse strains are not susceptible to RRV infection. In this report, we found that expression of IFN-λ may be a mechanistic basis for the susceptibility.

IFN-λ is a cytokine in the family of IFNs predominately found in cells of epithelial origin, which plays a role in innate immunity and host response to viral infection (Donnelly and Kotenko 2010). We found that RRV does not replicate as effectively in the extrahepatic bile ducts of C57BL/6 mice, which express higher constitutive levels of IFN-λ indicating that IFN-λ plays a role in host defense from RRV infection.

Primary cholangiocytes from BALB/c and C57BL/6 mice revealed significantly higher levels of IFN-λ in the C57BL/6 cholangiocytes both with SF media alone and after RRV infection, resulting in significantly lower viral replication titers. IFN-λ is a paracrine cytokine, which is released from epithelial cells when exposed to viral antigens or environmental stress, such as SF media. IFN-λ then signals surrounding cells, protecting them from subsequent infection (Ramos and others 2019; Ye and others 2019). This downstream protection may explain why viral titers in BALB/c primary cholangiocytes are equivalent to the C57BL/6 strain

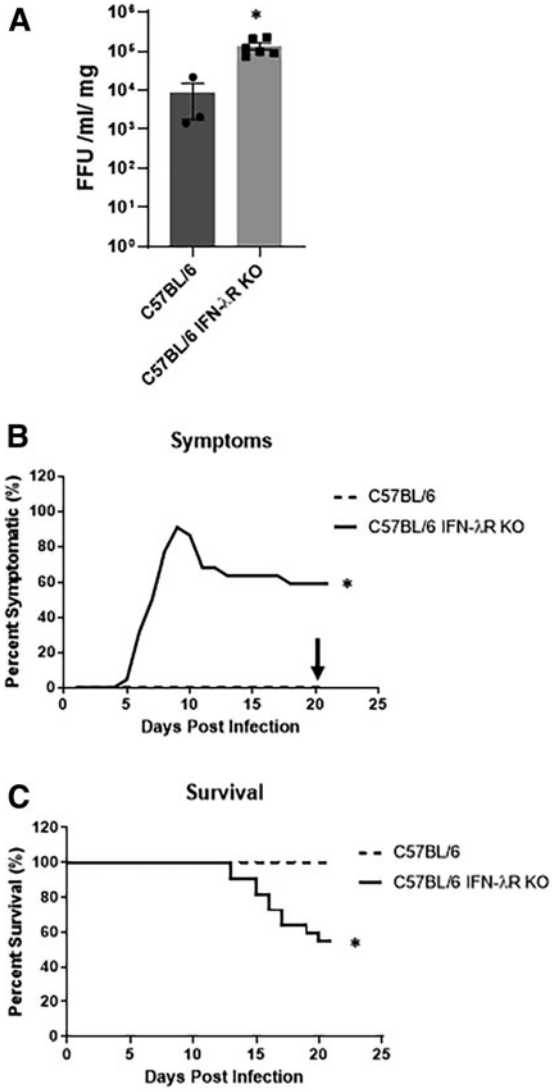

FIG. 5. RRV replication in bile duct, symptoms, and survival in C57BL/6 and C57BL/6 IFN-λR KO mice. **(A)** Viral titers were performed on bile ducts from 7 DPI C57BL/6 ($n=3$) and C57BL/6 IFN-λR KO mice ($n=6$) demonstrate 100-fold greater viral replication in C57BL/6 IFN-λR KO mice compared with C57BL/6 mice. Unpaired *t*-test $*P<0.05$. **(B)** After RRV infection, 90% of C57BL/6 IFN-λR KO mice ($n=22$) demonstrated obstructive symptoms compared to 0% of the C57BL/6 mice ($n=17$). Fisher's exact test $*P<0.05$. **(C)** C57BL/6 IFN-λR KO mice experience a reduction in survival with an estimated 45% mortality. Fisher's exact test $*P<0.05$. Circles represents C57BL/6. Squares represents C57BL/6 IFN-λR KO. IFN-λR KO, IFN-λ receptor knockout.

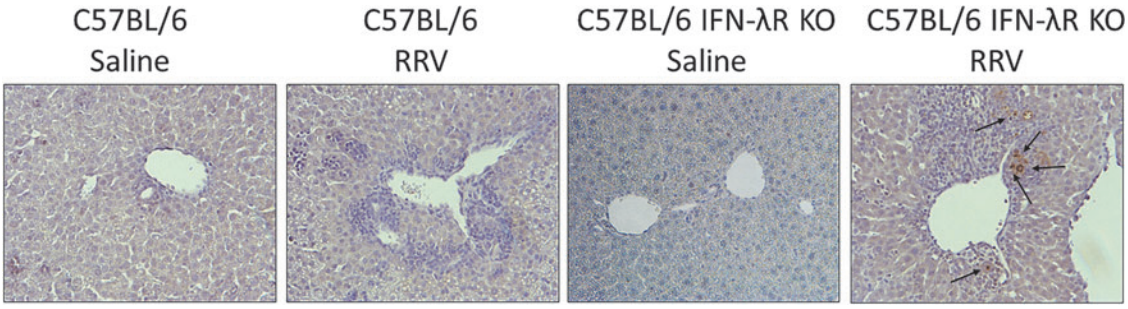

FIG. 6. Immunohistochemistry for detection of RRV antigens in liver sections of C57BL/6 and C57BL/6 IFN-λR KO mice. Immunohistochemistry performed on liver sections of 7 DPI injected pups demonstrate RRV antigen staining in the portal triads of C57BL/6 IFN-λR KO mice. The RRV is localized predominately around the portal triads. No virus is seen on C57BL/6 RRV staining (10×magnification).

at 24 h but increase 2.5-fold at 48 h, which is one replicative cycle of RRV (Jafri and others 2008). It is likely that the IFN-λ released from infected cells is sufficient to protect the neighboring cells against subsequent infection.

We next evaluated if knocking out the IFN-λR would induce susceptibility to a previously protected strain of mice, C57BL/6. When C57BL/6 IFN-λR KO mice were infected with RRV, 90% of pups developed obstructive symptoms and exhibited a significant reduction in survival at 21 days compared to C57BL/6 pups. RRV also replicated at significantly higher levels in the C57BL/6 IFN-λR KO mice in the extrahepatic bile ducts, demonstrating that the presence of IFN-λ is playing a significant role in the inhibition of RRV replication in the hepatobiliary tree. In addition, histology of the infected C57BL/6 IFN-λR KO mice revealed significant periportal inflammation and bile duct obstruction, similar to that seen in the BALB/c mouse line.

These findings indicate that IFN-λ is critical in the host defense against RRV infection. Deficiency in IFN-λ permits higher levels of RRV replication in the bile duct, which is sufficient to induce the inflammatory cascade leading to the murine model of BA. This lower baseline level of IFN-λ may explain why we have previously only been able to induce the murine BA model in the BALB/c mouse line. Though the full mechanism of RRV infection and the murine BA model is likely multifactorial, IFN-λ does appear to be a critical signaling protein-inhibiting RRV infection.

Though this has not been previously assessed, more study is needed on IFN-λ in humans, specifically neonates. There have been well-described genetic polymorphisms that affect cytokine production in newborns influencing their ability to fight infections. These include interleukin-1β and toll-like receptors (TLRs) in susceptibility to malaria as well as polymorphisms in TLR4 and increased vulnerability to neonatal sepsis (Mockenhaupt and others 2006; Natama and others 2021; Li and others 2022). If a cohort of newborn infants has lower baseline levels of IFN-λ, this may leave them vulnerable to viral pathogens and the sequelae of

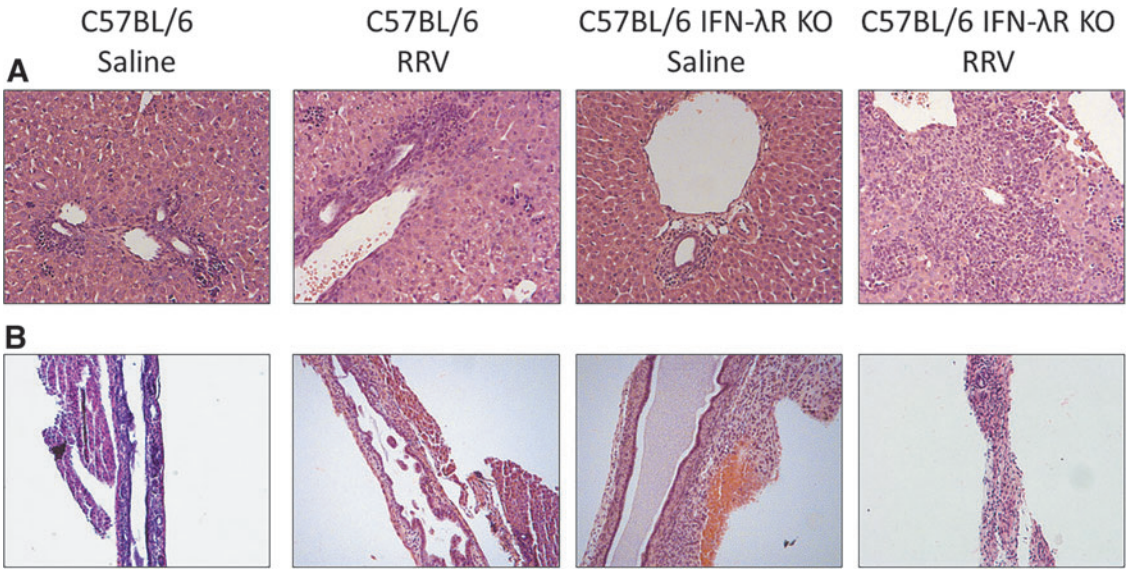

FIG. 7. H&E stain of **(A)** liver and **(B)** bile ducts in C57BL/6 and C57BL/6 IFN-λR KO Mice. H&E staining demonstrated significant periportal inflammation in the C57BL/6 IFN-λR KO mice after RRV infection. C57BL/6 mice had minimal inflammatory change. Extrahepatic bile ducts of 10 DPI mice were obstructed in the symptomatic C57BL/6 IFN-λR KO mice, whereas C57BL/6 bile ducts remained patent (10×magnification). H&E, hematoxylin, and eosin.

subsequent infection. Further studies are needed both for RRV's association with human BA and IFN-λ levels or IFN-λ gene polymorphisms in the first few weeks of infant life.

Acknowledgment

Ashley Cast provided technical assistance with Western blots.

Author Disclosure Statement

No competing financial interests exist.

Funding Information

This work was supported in part by National Institutes of Health (NIH) grants R01 DK-091566 (to G.M.T and S.K.M).

References

Allen SR, Jafri M, Donnelly B, McNeal M, Witte D, Bezerra J, Ward R, Tiao GM. 2007. Effect of rotavirus strain on the murine model of biliary atresia. J Virol 81(4):1671–1679.

Asai A, Miethke A, Bezerra JA. 2015. Pathogenesis of biliary atresia: defining biology to understand clinical phenotypes. Nat Rev Gastroenterol Hepatol 12(6):342–352.

Brand S, Beigel F, Olszak T, Zitzmann K, Eichhorst ST, Otte JM, Diebold J, Diepolder H, Adler B, Auernhammer CJ, Göke B, Dambacher J. 2005. IL-28A and IL-29 mediate antiproliferative and antiviral signals in intestinal epithelial cells and murine CMV infection increases colonic IL-28A expression. Am J Physiol Gastrointest Liver Physiol 289(5): G960–G968.

Davenport M. 2005. Biliary atresia. Semin Pediatr Surg 14(1): 42–48.

Davenport M, Gonde C, Redkar R, Koukoulis G, Tredger M, Mieli-Vergani G, Portmann B, Howard ER. 2001. Immunohistochemistry of the liver and biliary tree in extrahepatic biliary atresia. J Pediatr Surg 36(7):1017–1025.

Doldan P, Dai J, Metz-Zumaran C, Patton JT, Stanifer ML, Boulant S. 2022. Type III and not type I interferons efficiently prevent the spread of rotavirus in human intestinal epithelial cells. J Virol 96(17):e0070622.

Donnelly RP, Kotenko SV. 2010. Interferon-lambda: a new addition to an old family. J Interferon Cytokine Res 30(8): 555–564; doi:10.1089/jir.2010.0078

Elkins KL, Cooper A, Colombini SM, Cowley SC, Kieffer TL. 2002. In vivo clearance of an intracellular bacterium, *Francisella tularensis* LVS, is dependent on the p40 subunit of interleukin-12 (IL-12) but not on IL-12 p70. Infect Immun 70(4):1936–1948.

Erickson N, Mohanty SK, Shivakumar P, Sabla G, Chakraborty R, Bezerra JA. 2008. Temporal-spatial activation of apoptosis and epithelial injury in murine experimental biliary atresia. Hepatology 47(5):1567–1577.

Hermant P, Demarez C, Mahlakõiv T, Staeheli P, Meuleman P, Michiels T. 2014. Human but not mouse hepatocytes respond to interferon-lambda in vivo. PLoS One 9(1):e87906.

Hopkins PC, Yazigi N, Nylund CM. 2017. Incidence of biliary atresia and timing of hepatoportoenterostomy in the United States. J Pediatr 187:253–257.

Jafri M, Donnelly B, Allen S, Bondoc A, McNeal M, Rennert PD, Weinreb PH, Ward R, Tiao G. 2008. Cholangiocyte expression of alpha2beta1-integrin confers susceptibility to rotavirus-induced experimental biliary atresia. Am J Physiol Gastrointest Liver Physiol 295(1):G16–G26.

Jafri M, Donnelly B, Bondoc A, Allen S, Tiao G. 2009. Cholangiocyte secretion of chemokines in experimental biliary atresia. J Pediatr Surg 44(3):500–507.

Jewell NA, Cline T, Mertz SE, Smirnov SV, Flaño E, Schindler C, Grieves JL, Durbin RK, Kotenko SV, Durbin JE. 2010. Lambda interferon is the predominant interferon induced by influenza A virus infection in vivo. J Virol 84(21):11515–11522.

Kasai M. 1959. A new operation for ''non-correctable'' biliary atresia: hepatic portoenterostomy. Shujutsu 13:733–739.

Lakshminarayanan B, Davenport M. 2016. Biliary atresia: a comprehensive review. J Autoimmun 73:1–9.

Li M, Pan S, Chen H, Yan S, Liu Y. 2022. Effect of TLR-4 gene polymorphisms on sepsis susceptibility in neonates: a systematic review and meta-analysis. Biomark Med 16(13): 1005–1017.

Lin JD, Feng N, Sen A, Balan M, Tseng HC, McElrath C, Smirnov SV, Peng J, Yasukawa LL, Durbin RK, Durbin JE, Greenberg HB, Kotenko SV. 2016. Distinct roles of type I and type III interferons in intestinal immunity to homologous and heterologous rotavirus infections. PLoS Pathog 12(4): e1005600.

Mack CL, Falta MT, Sullivan AK, Karrer F, Sokol RJ, Freed BM, Fontenot AP. 2007. Oligoclonal expansions of CD4+ and CD8+ T-cells in the target organ of patients with biliary atresia. Gastroenterology 133(1):278–287.

Mahlakõiv T, Hernandez P, Gronke K, Diefenbach A, Staeheli P. 2015. Leukocyte-derived IFN-α/β and epithelial IFN-λ constitute a compartmentalized mucosal defense system that restricts enteric virus infections. PLoS Pathog 11(4): e1004782.

McNeal MM, Broome RL, Ward RL. 1994. Active immunity against rotavirus infection in mice is correlated with viral replication and titers of serum rotavirus IgA following vaccination. Virology 204(2):642–650.

Mills CD, Kincaid K, Alt JM, Heilman MJ, Hill AM. 2000. M-1/M-2 macrophages and the Th1/Th2 paradigm. J Immunol 164(12):6166–6173.

Mockenhaupt FP, Cramer JP, Hamann L, Stegemann MS, Eckert J, Oh NR, Otchwemah RN, Dietz E, Ehrhardt S, Schröder NW, Bienzle U, Schumann RR. 2006. Toll-like receptor (TLR) polymorphisms in African children: common TLR-4 variants predispose to severe malaria. Proc Natl Acad Sci U S A 103(1):177–182.

Mohanty SK, Donnelly B, Bondoc A, Jafri M, Walther A, Coots A, McNeal M, Witte D, Tiao GM. 2013. Rotavirus replication in the cholangiocyte mediates the temporal dependence of murine biliary atresia. PLoS One 8(7):e69069.

Mohanty SK, Donnelly B, Temple H, Tiao GM. 2019. A rotavirus-induced mouse model to study biliary atresia and neonatal cholestasis. Methods Mol Biol 1981:259–271.

Mohanty SK, Lobeck I, Donnelly B, Dupree P, Walther A, Mowery S, Coots A, Bondoc A, Sheridan RM, Poling HM, Temple H, McNeal M, Sestak K, Bansal R, Tiao G. 2020. Rotavirus reassortant-induced murine model of liver fibrosis parallels human biliary atresia. Hepatology 71(4):1316–1330.

Muzammil, Jayanthi D, Faizuddin M, Noor Ahamadi HM. 2017. Association of interferon lambda-1 with herpes simplex viruses-1 and -2, Epstein-Barr virus, and human cytomegalovirus in chronic periodontitis. J Investig Clin Dent 8(2):e12200.

Natama HM, Rovira-Vallbona E, Krit M, Guetens P, Sorgho H, Somé MA, Traoré-Coulibaly M, Valéa I, Mens PF, Schallig

H, Berkvens D, Kestens L, Tinto H, Rosanas-Urgell A. 2021. Genetic variation in the immune system and malaria susceptibility in infants: a nested case-control study in Nanoro, Burkina Faso. Malar J 20(1):94.

Ohya T, Fujimoto T, Shimomura H, Miyano T. 1995. Degeneration of intrahepatic bile duct with lymphocyte infiltration into biliary epithelial cells in biliary atresia. J Pediatr Surg 30(4):515–518.

Ramos I, Smith G, Ruf-Zamojski F, Martínez-Romero C, Fribourg M, Carbajal EA, Hartmann BM, Nair VD, Marjanovic N, Monteagudo PL, DeJesus VA, Mutetwa T, Zamojski M, Tan GS, Jayaprakash C, Zaslavsky E, Albrecht RA, Sealfon SC, García-Sastre A, Fernandez-Sesma A. 2019. Innate immune response to influenza virus at single-cell resolution in human epithelial cells revealed paracrine induction of interferon lambda 1. J Virol 93(20):e00559-19.

Riepenhoff-Talty M, Schaekel K, Clark HF, Mueller W, Uhnoo I, Rossi T, Fisher J, Ogra PL. 1993. Group A rotaviruses produce extrahepatic biliary obstruction in orally inoculated newborn mice. Pediatr Res 33(4 Pt 1):394–399.

Sanchez-Valle A, Kassira N, Varela VC, Radu SC, Paidas C, Kirby RS. 2017. Biliary atresia: epidemiology, genetics, clinical update, and public health perspective. Adv Pediatr 64(1):285–305.

Santos CS, Macedo JO, Bandeira M, Chagas-Junior AD, McBride AJA, McBride FWC, Reis MG, Athanazio DA. 2010. Different outcomes of experimental leptospiral infection in mouse strains with distinct genotypes. J Med Microbiol 59(Pt 9):1101–1106.

Sellers RS, Clifford CB, Treuting PM, Brayton C. 2012. Immunological variation between inbred laboratory mouse strains: points to consider in phenotyping genetically immunomodified mice. Vet Pathol 49(1):32–43.

Shivakumar P, Campbell KM, Sabla GE, Miethke A, Tiao G, McNeal MM, Ward RL, Bezerra JA. 2004. Obstruction of extrahepatic bile ducts by lymphocytes is regulated by IFN-gamma in experimental biliary atresia. J Clin Invest 114(3): 322–329.

Simpson EM, Linder CC, Sargent EE, Davisson MT, Mobraaten LE, Sharp JJ. 1997. Genetic variation among 129 substrains and its importance for targeted mutagenesis in mice. Nat Genet 16(1):19–27.

Tyler KL, Sokol RJ, Oberhaus SM, Le M, Karrer FM, Narkewicz MR, Tyson RW, Murphy JR, Low R, Brown WR. 1998. Detection of reovirus RNA in hepatobiliary tissues from patients with extrahepatic biliary atresia and choledochal cysts. Hepatology 27(6):1475–1482.

Ye L, Schnepf D, Staeheli P. 2019. Interferon-λ orchestrates innate and adaptive mucosal immune responses. Nat Rev Immunol 19(10):614–625.

Yoon PW, Bresee JS, Olney RS, James LM, Khoury MJ. 1997. Epidemiology of biliary atresia: a population-based study. Pediatrics 99(3):376–382.

Zani A, Quaglia A, Hadzić N, Zuckerman M, Davenport M. 2015. Cytomegalovirus-associated biliary atresia: an aetiological and prognostic subgroup. J Pediatr Surg 50(10):1739–1745.

Address correspondence to:
Dr. Greg M. Tiao
Department of Pediatric and Thoracic Surgery
Cincinnati Children's Hospital Medical Center
3333 Burnet Avenue, MLC 2023
Cincinnati, OH 45229
USA

E-mail: greg.tiao@cchmc.org

Received 31 March 2023/Accepted 1 August 2023